



Massive black hole and Population III galaxy formation in over-massive dark matter halos with violent merger histories

Kohei Inayoshi¹  , Miao Li² and Zoltán Haiman¹

¹*Department of Astronomy, Columbia University, 550 W. 120th Street, New York, NY 10027, USA,*

²*Center for Computational Astrophysics, Flatiron Institute, 162 Fifth Avenue, New York, NY 10010, USA*

9 March 2024

ABSTRACT

We propose the formation of massive pristine dark-matter (DM) halos with masses of $\sim 10^8 M_\odot$, due to the dynamical effects of frequent mergers in rare regions of the Universe with high baryonic streaming velocity relative to DM. Since the streaming motion prevents gas collapse into DM halos and delays prior star formation episodes, the gas remains metal-free until the halo virial temperatures $\gtrsim 2 \times 10^4$ K. The minimum cooling mass of DM halos is boosted by a factor of $\sim 10 - 30$ because frequent major mergers of halos further inhibit gas collapse. We use Monte Carlo merger trees to simulate the DM assembly history under a streaming velocity of twice the root-mean-square value, and estimate the number density of massive DM halos containing pristine gas as $\simeq 10^{-4} \text{ cMpc}^{-3}$. When the gas infall begins, efficient Ly α cooling drives cold streams penetrating inside the halo and feeding a central galactic disc. When one stream collides with the disc, strong shock forms a dense and hot gas cloud, where the gas never forms H₂ molecules due to effective collisional dissociation. As a result, a massive gas cloud forms by gravitational instability and collapses directly into a massive black hole (BH) with $M_\bullet \sim 10^5 M_\odot$. Almost simultaneously, a galaxy with $M_{\star, \text{tot}} \sim 10^6 M_\odot$ composed of Population III stars forms in the nuclear region. If the typical stellar mass is as high as $\sim 100 M_\odot$, the galaxy could be detected with the *James Webb Space Telescope* even at $z \gtrsim 15$. These massive seed BHs would be fed by continuous gas accretion from the host galaxy, and grow to be bright quasars observed at $z \gtrsim 6$.

Key words: quasars: supermassive black holes – dark ages, reionization, first stars – stars: Population III – galaxies: formation

1 INTRODUCTION

The origin of supermassive black holes (SMBHs), which are ubiquitous at the centers of galaxies, is one of the most challenging puzzles in astrophysics. Observations in recent decades have revealed that SMBHs with masses of $M_\bullet \gtrsim 10^9 - 10^{10} M_\odot$ have already formed only within one billion years after the Big Bang (Fan 2006; Willott et al. 2010; Mortlock et al. 2011; Wu et al. 2015; Jiang et al. 2016; Matsuoka et al. 2016, 2018; Bañados et al. 2018). The existence of such monster SMBHs in the early Universe requires rapid formation and growth processes of BHs (Volonteri 2012; Haiman 2013; Johnson & Haardt 2016, and reference therein).

In this paper, we consider the formation of massive seed BHs (Loeb & Rasio 1994; Eisenstein & Loeb 1995; Oh & Haiman 2002; Koushiappas et al. 2004; Begelman et al. 2006; Lodato & Natarajan 2006; Mayer et al. 2010), where a supermassive star (SMS) with $\gtrsim 10^5 M_\odot$ formed in a protogalaxy collapses directly into a massive BH seed via general relativistic instability (Shibata & Shapiro 2002; Montero et al. 2012; Uchida et al. 2017). SMS formation can be achieved in an H₂-free pristine gas cloud with an almost constant and high temperature of $\sim 10^4$ K. Such a self-gravitating cloud collapses into a single star or several clumps due to fragmentation at the center of the halo (Regan et al. 2014; Inayoshi et al. 2014; Becerra et al. 2015; Latif et al. 2016a; Chon et al. 2018). Most of massive clumps would migrate inward and merge rapidly due to gravitational interaction with the surrounding gas disc (Inayoshi & Haiman 2014; Sakurai et al. 2016a). Since the hot gas envelope accretes on

* E-mail: inayoshi@astro.columbia.edu

† Simons Society of Fellows, Junior Fellow

the central protostar at a high rate of

$$\dot{M} \sim \frac{c_s^3}{G} \simeq 0.18 M_\odot \text{ yr}^{-1} \left(\frac{T}{10^4 \text{ K}} \right)^{3/2}, \quad (1)$$

(Larson 1969; Penston 1969; Shu 1977), the star can grow to an SMS with $M_\star \gtrsim 10^5 M_\odot$ within the lifetime of ~ 1 Myr. Because of rapid entropy input by accretion, the protostar has a bloated stellar envelope with an effective temperature of ~ 5000 K, which is much lower than that of normal massive stars (Hosokawa et al. 2012). Thus, the accreting protostar is unlikely to suffer either from radiation feedback or from pulsation-driven mass loss, and eventually collapses into a massive BH with $M_\bullet \gtrsim 10^5 M_\odot$ (Inayoshi et al. 2013; Hosokawa et al. 2013; Umeda et al. 2016; Haemmerlé et al. 2017). Such a massive seed could grow up to $\gtrsim 10^9 M_\odot$ through subsequent gas accretion by $z \gtrsim 6 - 7$ (e.g., Di Matteo et al. 2012; Smidt et al. 2017).

So far, H_2 dissociation by Lyman-Werner (LW) photons emitted from nearby star-forming galaxies has been mainly discussed in order to form massive seed BHs. In this scenario, intense LW radiation is required to prevent H_2 formation (e.g., Omukai 2001; Bromm & Loeb 2003; Shang et al. 2010; Inayoshi & Omukai 2011; Wolcott-Green et al. 2011; Johnson et al. 2013; Latif et al. 2014; Sugimura et al. 2014; Agarwal & Khochfar 2015; Chon et al. 2016; Wolcott-Green et al. 2017). The critical LW intensity (in units of $10^{-21} \text{ erg s}^{-1} \text{ cm}^{-2} \text{ Hz}^{-1}$) is estimated as $J_{\text{LW},21} \sim 10^3$, assuming that radiation sources have the same spectra as in metal-poor galaxies (Sugimura et al. 2014). Wolcott-Green et al. 2017 have improved the estimate considering optically-thick H_2 photo-dissociation rates over all the LW lines self-consistently with the spectra of source galaxies, though most other work just adopted a shielding factor instead. As a natural outcome, such star-forming galaxies are also likely to produce intense X-rays due to the existence of high-mass X-ray binaries and supernova explosions. However, X-ray ionization promotes H_2 formation through the electron-catalyzed reactions (Haiman, Rees & Loeb 1996), and thus the critical LW intensity for H_2 dissociation is boosted (Inayoshi & Omukai 2011; Latif et al. 2015; Inayoshi & Tanaka 2015; Glover 2016). As a result of this, the X-ray emission could invalidate the formation of massive seed BHs in the majority of halos exposed to LW radiation with $J_{\text{LW},21} > 10^3$.

Alternatively, H_2 collisional dissociation ($\text{H} + \text{H}_2 \rightarrow 3\text{H}$) potentially plays an important role in the formation of massive seed BHs in dense and hot shock regions satisfying

$$\left(\frac{n}{10^4 \text{ cm}^{-3}} \right) \left(\frac{T}{10^4 \text{ K}} \right) \gtrsim 1 \quad (2)$$

(Inayoshi & Omukai 2012), where n and T are the density and temperature of the shock gas. The shocked gas is expected to form by colliding accretion flows in the assembly of atomic-cooling halos with virial temperature of $T_{\text{vir}} \gtrsim 8000$ K. However, Fernandez et al. (2014) found that for halos with masses and virial temperatures near the atomic-cooling threshold ($\sim 10^4$ K), cold gas flows accrete into the halo but experience shocks before reaching the central region. In this case, the shocked gas is not dense enough to dissociate H_2 . This happens because the dynamical timescale of the flow is comparable to the radiative cooling timescale ($t_{\text{dyn}} \sim t_{\text{cool}}$). Visbal et al. (2014) have con-

firmed that dense shocked gas never forms without radiative cooling ($t_{\text{dyn}} \ll t_{\text{cool}}$)¹. Therefore, we require *more massive* haloes with $T_{\text{vir}} \gtrsim 10^4$ K, where the shock-dissipated energy is quickly carried away by radiative cooling. Since the atomic hydrogen cooling rate Λ_{H} depends steeply on the gas temperature ($\Lambda_{\text{H}} \propto T^\beta$ where $\beta \sim 8$ at $8000 \lesssim T/\text{K} \lesssim 2 \times 10^4$, and Λ_{H} has a peak value at $T \simeq 2 \times 10^4$ K), one can expect that the gas properties in massive DM halos with $T_{\text{vir}} \gtrsim 10^4$ K would change significantly due to radiative cooling. Analytical models and numerical simulations for lower-redshift and more massive galaxies with $T_{\text{vir}} \gg 10^4$ K suggest that cold streams can penetrate inside the halo and form shocks near the center (Birnboim & Dekel 2003; Dekel & Birnboim 2006; Dekel et al. 2009a, see also e.g., Rees & Ostriker 1977; White & Rees 1978; White & Frenk 1991).

One important concern is that such massive halos with $T_{\text{vir}} > 10^4$ K would be likely polluted by metals due to stellar activity in their progenitors. Metal pollution allows additional cooling by C/O lines and dust emission, leading to efficient gas fragmentation and suppressing SMS formation (Omukai et al. 2008; Inayoshi & Omukai 2012; Latif et al. 2016b)². To avoid metal pollution in massive halos, we here consider the effect of baryonic streaming motion (BSM) induced at the cosmological recombination epoch (Tselikhovich & Hirata 2010). The BSM is a natural mechanism suppressing gas collapse into halos and delaying formation of the first generation stars (Population III, hereafter PopIII) in mini-halos at $z > 15$ (Greif et al. 2011; Stacy et al. 2011; Fialkov et al. 2012). Applying the effect of high streaming velocities in semi-analytical merger-tree calculations, Tanaka & Li (2014) have found that star formation episodes can be suppressed, and the gas is kept pristine until the halo virial temperatures reach ~ 8000 K at $z \gtrsim 30$ ³. Hirano et al. (2017) have found that a high gas accretion rate of $\dot{M} \gtrsim 10^{-2} M_\odot \text{ yr}^{-1}$ onto the center of a massive halo under strong BSM would be realized. Recent cosmological simulations by Schauer et al. (2017) suggest that in a rare patch of the Universe with strong BSM, star formation is suppressed, even more efficiently than expected in Tanaka & Li (2014). Another simulation result by Hirano et al. (2018) suggests that *dynamical effects due to frequent mergers of gaseous halos violently disturb the collapsing region and further prevent star formation*. As a result, star formation can be quenched until DM halos become as massive as $\simeq 10^8 M_\odot$ ($T_{\text{vir}} \gtrsim 2 \times 10^4$ K at $15 < z < 20$), which is $\gtrsim 10$ times more massive than the minimum cooling mass in a region having strong BSM, estimated by the previous

¹ One possible idea proposed by Inayoshi, Visbal & Kashiyama (2015) is a high-velocity collision of two DM haloes with a relative velocity $\gtrsim 200 \text{ km s}^{-1}$, inside which star formation has not occurred yet because of lower densities ($n \sim 10^2 \text{ cm}^{-3}$). The shocked gas due to such a violent galaxy collision heats up to $\sim 10^6$ K and cools isobarically via free-free emission and He/H lines, resulting in dense gas with $n \gtrsim 10^4 \text{ cm}^{-3}$ at $T \sim 10^4$ K.

² Alternatively, Mayer et al. (2015) have proposed that in a very massive halo with $M_{\text{vir}} \simeq 10^{12} M_\odot$ at $z \sim 10$ ($T_{\text{vir}} \sim 10^7$ K), shock heating driven by intense inflows could prevent gas fragmentation even in the face of the metal-line cooling.

³ The total gas mass is $\sim 7 \times 10^5 M_\odot (T_{\text{vir}}/8000 \text{ K})^{3/2} [(1+z)/31]^{-3/2}$. Thus, this fact requires a large fraction of the total mass to be converted into a single SMS with $M_\star > 10^5 M_\odot$.

work (Greif et al. 2011; Stacy et al. 2011; Fialkov et al. 2012; Tanaka & Li 2014). In a massive pristine DM halo, more efficient cooling can induce deeper penetration of cold accretion flows (e.g., Fernandez et al. 2014, and see §4.2.2), and form dense shocks where a massive seed BH would be initiated.

Massive pristine DM halos with $\simeq 10^8 M_\odot$ not only form a massive seed BH, but also form bright galaxies with $\simeq 10^6 M_\odot$ dominated by PopIII stars. In previous work, formation of PopIII clusters/galaxies in halos with $\sim 10^8 M_\odot$ has been discussed, considering strong ionizing radiation to stall gas collapse into halos instead of strong BSM (Johnson 2010; Yajima & Khochfar 2017; Visbal et al. 2017). However, the number density of massive PopIII galaxies is expected to be $\sim 10^{-7} \text{ Mpc}^{-3}$ at $z \sim 7$ (Visbal et al. 2017), which seems too rare to be observed by the *James Webb Space Telescope* (*JWST*). In contrast, the BSM effect enhances the number density of PopIII galaxies at $z > 10$ by several orders of magnitude because DM halos under streaming velocity with twice the root-mean-square value are not as rare as DM halos exposed to very bright and synchronously forming ionizing neighbors. This result strongly motivates us to explore PopIII galaxies with *JWST*.

This paper is organized as follows. In §2, we describe the method to study the suppression of star formation in massive DM halos in rare patches of the Universe with high streaming velocity and unusual merger histories with frequent major merger events. In §3, we discuss the necessary conditions required to form massive seed BHs in dense and hot shock regions produced at the interface between cold streams and a galactic disc, and discuss the detectability of massive Pop III galaxies with *JWST*. Finally, we discuss several caveats in §4 and summarize our conclusions in §5. Throughout this paper, we assume a CDM cosmology consistent with Planck Collaboration XVI et al. (2014): $\Omega_m = 0.32$, $\Omega_\Lambda = 0.68$, $\Omega_b = 0.049$, $h = 0.67$, $\sigma_8 = 0.83$ and $n_s = 0.96$.

2 VIOLENT MERGERS ENHANCE THE MASS OF PRISTINE ATOMIC-COOLING HALOS UNDER HIGH STREAMING VELOCITIES

We consider a massive DM halo with a virial temperature of $T_{\text{vir}} \gtrsim 10^4 \text{ K}$ at high redshift. The virial mass, the virial radius and the circular velocity of the halo are given by

$$M_{\text{vir}} \simeq 1.7 \times 10^7 T_{\text{vir},4}^{3/2} M_\odot \left(\frac{1+z}{16} \right)^{-3/2}, \quad (3)$$

$$R_{\text{vir}} \simeq 350 h^{-1} T_{\text{vir},4}^{1/2} \text{ pc} \left(\frac{1+z}{16} \right)^{-3/2}, \quad (4)$$

and

$$V_{\text{vir}} = \sqrt{\frac{GM_{\text{vir}}}{R_{\text{vir}}}} \simeq 12 T_{\text{vir},4}^{1/2} \text{ km s}^{-1} \quad (5)$$

(Bryan & Norman 1998).

We here consider a rare patch of the Universe where BSM suppresses star formation episodes in the progenitor halos. The streaming velocity v_{bsm} follows a Maxwell-Boltzmann distribution with the root-mean-square speed of $\sigma_{\text{bsm}} \sim 30 \text{ km s}^{-1}$ at $z_{\text{rec}} \simeq 1100$, and decays as $\tilde{v}_{\text{bsm}}(z) =$

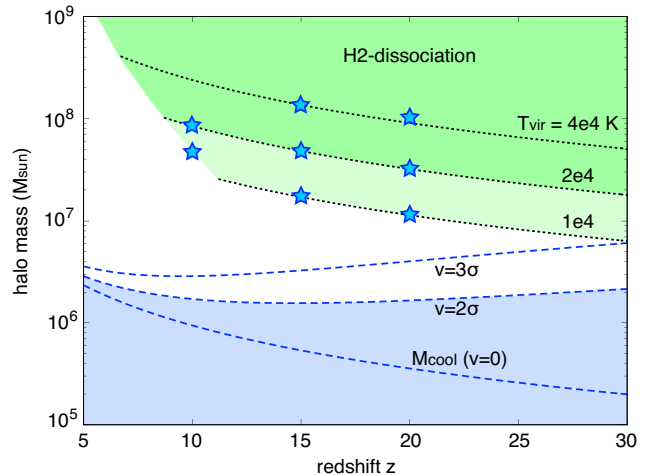


Figure 1. Evolution of characteristic DM halo masses. Dashed curves (blue) show the critical halo masses above which the gas can collapse into the halo, for three different streaming velocities v_{bsm} . In the green region, H_2 is collisionally dissociated if dense shocks form at the edge of the galactic disc (see Eq. 20). Dotted curves indicate constant virial temperatures, the values of which are denoted by numbers in the figure. The critical virial temperature required for deep penetration of cold streams is set to $T_{\text{vir}} \geq 2 \times 10^4 \text{ K}$ (see §3.2). Stars show the masses and redshifts of DM halos we simulated with merger trees (see Table 1). The gas between the blue and green regions can be bridged by halos with unusually frequent merging histories.

$v_{\text{bsm}}[(1+z)/(1+z_{\text{rec}})]$ toward lower redshift (e.g., Tselikovich & Hirata 2010). Because of the BSM, star formation in mini-halos with $M_{\text{vir}} \lesssim 10^6 M_\odot$ is significantly delayed until $z < 10$. Fialkov et al. (2012) fitted the critical circular velocity of DM halos above which the gas can collapse as

$$v_{\text{cool}} = \sqrt{v_0^2 + [\alpha \tilde{v}_{\text{bsm}}(z)]^2}, \quad (6)$$

where the two parameters are estimated as $(v_0, \alpha) \simeq (3.7 \text{ km s}^{-1}, 4)$, based on the results with cosmological simulations for PopIII formation in mini-halos (Greif et al. 2011; Stacy et al. 2011). Using Eq. (6), the critical halo mass for cooling is given by

$$M_{\text{cool}}(v_{\text{bsm}}, z) = 1.9 \times 10^6 M_\odot \left(\frac{1+z}{16} \right)^{-3/2} \times \left[0.43 + \left(\frac{v_{\text{bsm}}}{3\sigma_{\text{bsm}}} \right)^2 \left(\frac{1+z}{16} \right)^2 \right]^{3/2}. \quad (7)$$

Note that those simulations considered either weak BSM $v_{\text{bsm}} \simeq \sigma_{\text{bsm}}$ or an isolated DM halo (i.e., a small simulation box). In Fig. 1, we show the critical masses $M_{\text{cool}}(v_{\text{bsm}}, z)$ for three different streaming velocities (blue dashed curves).

Recently, Schauer et al. (2017) have studied the effect of a high streaming velocity with $v_{\text{bsm}} = 3\sigma_{\text{bsm}}$ considering a large simulation box ($64 h^{-3} \text{ Mpc}^3$), and found that the gas in DM halos less massive than $\simeq 2 \times 10^7 M_\odot$ can neither collapse nor form stars. Similarly, Hirano et al. (2018) concluded that in a rare patch of the Universe with $v_{\text{bsm}} \gtrsim 2\sigma_{\text{bsm}}$, the first collapsing object (with gas) is as massive as $\gtrsim 3 \times 10^7 M_\odot$ at $15 \lesssim z \lesssim 20$. The virial temperature

of the halo is $T_{\text{vir}} \gtrsim 2 \times 10^4$ K. These critical masses found by their cosmological simulations are $\gtrsim 10$ times higher than $M_{\text{cool}}(v_{\text{bsm}} \gtrsim 2\sigma_{\text{bsm}}, z)$, shown in Fig. 1.

The existence of the mass gap implies that additional effects suppress gas collapse even if the halo mass exceeds the minimum cooling mass. Hirano et al. (2018) have pointed out that frequent merger events of DM halos containing gas violently disturb the central collapsing core in the main progenitor, as shown in their Figure 2. Motivated by this, we here discuss how likely such violent mergers can quench star formation further and close the mass gap. For this purpose, we use the Monte Carlo merger trees to simulate the assembly history of DM halos of interest. The algorithm of merger trees is detailed in Tanaka et al. (2013): the formation of DM halos is based on the ellipsoidal collapse model (Sheth & Tormen 2002) under the extended Press-Schechter formalism. When compared with cosmological N-body simulations, the ellipsoidal model is better than the spherical model in predicting the number of most massive halos for large look-back times. The algorithm of the merger tree is the ‘‘method B’’ in Zhang et al. (2008). In this algorithm, the time step Δz for the merger tree can be chosen freely. We choose $\Delta z = 0.02$ in this paper.

We have selected several atomic-cooling DM halos, with masses and redshifts (M_0, z_0). For each merger tree of these halos, we keep track of all the progenitors with masses above M_{cool} . We are looking for the *pristine trees* that satisfies the following criteria: none of the progenitors have gas collapse. This requires that every progenitor above M_{cool} has major mergers frequently enough that the redshift interval between two consecutive major mergers is shorter than the timescale of star formation, $\Delta z_{\text{m}} < \Delta z_{\text{col}}$ (see Eq. 8 below). We here define major mergers as ones with progenitor mass ratio of $f_{\text{m}} \equiv M_1/(M_1 + M_2) \geq 1/4$ (i.e., $M_1 \geq M_2/3$), where M_1 and $M_2 (\geq M_1)$ are masses of DM halos that undergo mergers. For example, suppose a major merger occurring at redshift z_1 . Then the progenitors of this event should experience another prior major mergers within $[z_1, z_1 + \Delta z_{\text{col}}(z_1)]^4$, otherwise this tree is counted as a *metal-polluted tree* due to star formation. We keep the simulation until all the progenitors are below M_{cool} , or until the tree becomes metal-polluted. Eventually, this calculation gives us the probability of pristine trees, $\mathcal{P}_{Z=0}$, for the parent halo with M_0 and z_0 . For each of these halos, we have many realizations of its merger trees, $N_{\text{tree}} \sim O(10^4 - 10^6)$, so that the statistical errors become smaller than 0.1 $\mathcal{P}_{Z=0}$.

In order to obtain Δz_{col} , we here estimate the timescale of star formation as

$$\Delta z_{\text{col}} = C \sqrt{\frac{3\pi}{32G\bar{\rho}_{\text{m}}(z)\Delta_{\text{vir}}}}, \quad (8)$$

where $\bar{\rho}_{\text{m}}(z)$ is the mean mass density (DM+gas) at redshift z , $\Delta_{\text{vir}} \simeq 18\pi^2$ is the over-density relative to the cosmic mean value at the collapse redshift. We note that the expression of $t_{\text{ff}}(\rho) = \sqrt{3\pi/(32G\rho)}$ is the free-fall timescale of an initially static and uniform medium with a mean density ρ . The actual collapse timescale of the cloud is longer than

⁴ In principle, the interval should be $[z_1, z_2]$, where z_2 is obtained from $z_2 = z_1 + \Delta z_{\text{col}}(z_2)$. But in practice, this is a second-order effect and makes little difference to the results.

Table 1. Results of merger-tree simulations

v_{bsm}	$T_{\text{vir},4}$	$M_{0,7}$	z_0	$\mathcal{P}_{Z=0}$	\mathcal{N} (cMpc $^{-3}$)
60	1.0	1.13	20	0.44	2.5×10^{-3}
60	1.0	1.70	15	0.11	2.7×10^{-3}
60	1.4	4.70	10	4.4×10^{-5}	3.2×10^{-6}
60	2.0	3.2	20	0.12	2.3×10^{-4}
60	2.0	4.8	15	4.8×10^{-3}	5.8×10^{-5}
60	2.0	8.4	10	$< 5.0 \times 10^{-7}$	$< 1.8 \times 10^{-8}$
60	4.3	10	20	4.9×10^{-3}	1.0×10^{-6}
60	4.0	14	15	6.0×10^{-6}	1.0×10^{-8}
30	2.0	4.8	15	4.0×10^{-6}	2.6×10^{-6}
90	2.0	4.8	15	8.9×10^{-2}	8.0×10^{-7}
60*	2.0	4.8	15	5.7×10^{-5}	7.0×10^{-7}

Column: (1) streaming velocity in unit of km s^{-1} ($\sigma_{\text{bsm}} = 30 \text{ km s}^{-1}$), (2) virial temperature in unit of 10^4 K, (3) DM halo mass in unit of $10^7 M_{\odot}$, (4) redshift for DM halos we simulate, (5) the fraction of merger trees in which the gas is kept pristine due to violent major mergers, $\mathcal{P}_{Z=0}$, and (6) their number density, $\mathcal{N} \equiv f_{\text{v}} \mathcal{P}_{Z=0} (dn_{\text{h}}/d \ln M_{\text{vir}})$. We adopt $C = 1.5$ to characterize the star formation timescale (Eq. 8), calibrated based on simulations by Hirano et al. (2018) (see text). In the last row (*), we set $C = 1$ to show the lowest probability.

that for pressure-free collapse t_{ff} . The factor $C (> 1)$ characterizes the delay of collapse due to the gas pressure gradient force and residual of BSM. When an isothermal cloud in a hydrostatic equilibrium collapses, the collapse timescale becomes longer than the free-fall one and thus $C \simeq 2 - 3$ (Foster & Chevalier 1993; Tsuribe & Inutsuka 1999; Aikawa et al. 2005). Assuming that a major merger occurs at z , the redshift interval where gas collapse stalls is estimated as

$$\frac{\Delta z_{\text{col}}}{1+z} = \left[1 - \left\{ 1 + \frac{\Delta t_{\text{col}}(z)}{t_{\text{H}}(z)} \right\}^{-2/3} \right] \equiv D, \quad (9)$$

where the ratio of $\Delta t_{\text{col}}(z)$ to the Hubble timescale $t_{\text{H}}(z)$ does not depend on redshift as

$$\frac{\Delta t_{\text{col}}(z)}{t_{\text{H}}(z)} = \frac{C}{4\sqrt{2}}. \quad (10)$$

We define the redshift when gas can collapse unless next major mergers occur as $\bar{z} \equiv z - \Delta z_{\text{col}}$. Thus, the redshift interval is rewritten as

$$\Delta z_{\text{col}} = \frac{D(1+\bar{z})}{1-D} \simeq (1+\bar{z}) \times \begin{cases} 0.12 & (C=1), \\ 0.17 & (C=1.5), \\ 0.22 & (C=2). \end{cases} \quad (11)$$

In the merger-tree calculations, where we are looking at the history backward, we adopt Eq.(11) setting $\bar{z} = z_1$. Taking the results from cosmological simulations by Hirano et al. (2018), where two DM halos are studied for $v_{\text{bsm}} \geq 2 \sigma_{\text{bsm}}$, the delay-timescale of star formation is $\Delta z_{\text{col}} \sim 2 - 4$ at $15 \lesssim \bar{z} \lesssim 23$, which allows us to adopt $C \simeq 1.5$ as our fiducial value, calibrated by these simulations. We note that in the simulations by Hirano et al. (2018), the density at the central core ($\lesssim 0.1 R_{\text{vir}}$) before collapse is as high as $\gtrsim 10^2 \text{ cm}^{-3}$, where the free-fall timescale is much shorter than that we consider. However, the dense core cannot be gravitationally unstable until gas at larger scales $\sim R_{\text{vir}}$ begins to collapse.

Table 2. Same as Table 1 but for different criteria for characterizing major mergers of DM halos

f_{cr}	mass ratio	$\mathcal{P}_{Z=0}$	\mathcal{N} (cMpc $^{-3}$)
0.15	1 : 5.67	5.4×10^{-2}	6.5×10^{-4}
0.2	1 : 4	1.6×10^{-2}	1.9×10^{-4}
0.25	1 : 3	4.8×10^{-3}	5.8×10^{-5}
0.3	1 : 2.33	1.5×10^{-3}	1.8×10^{-5}

Major mergers are defined as ones with progenitor mass fraction of $f_m \geq f_{\text{cr}}$, where $f_m \equiv M_1/(M_1 + M_2)$ and $M_1 \leq M_2$. We show the results for $T_{\text{vir}} = 2 \times 10^4$ K, $M_0 = 4.8 \times 10^7 M_\odot$, $z_0 = 15$ and $v_{\text{bsm}} = 60 \text{ km s}^{-1}$. The fraction of pristine trees is fitted by $\mathcal{P}_{Z=0} = \exp(-Af_{\text{cr}} + B)$, where $A = 23.85$ and $B = 0.64$.

Thus, the dense core can be disrupted by major mergers, and then takes longer to reform (i.e. the collapse time at the mean halo density).

In Fig. 2 and Table. 1, we summarize the results of the merger-tree simulations for our fiducial case ($C = 1.5$). For a given DM halo with M_0 and z_0 , we calculate the fraction of merger trees $\mathcal{P}_{Z=0}$ that keep the gas pristine due to violent major mergers even after the masses of the all progenitors exceed the minimum cooling mass M_{cool} . As shown in Fig. 2 (a), the fraction of pristine DM halos increases for lower T_{vir} or higher z_0 (i.e., lower M_0) because the mass gap between M_{cool} and M_0 becomes smaller (see the blue and green hatched regions in Fig. 1). For higher T_{vir} or lower z_0 (i.e., higher M_0), the probability drops sharply because the mass gap becomes bigger. Combined with the mass function of DM halos (Sheth & Tormen 2002), we can estimate the number density of DM halos containing pristine gas as

$$\mathcal{N} = f_{2\sigma} \mathcal{P}_{Z=0} \frac{dn_h}{d \ln M_{\text{vir}}}, \quad (12)$$

where the fraction of the Universe with streaming velocities of $v_{\text{bsm}} \geq 2\sigma_{\text{bsm}}$ is $f_{2\sigma} \simeq 8 \times 10^{-3}$. Note that the coherence length of the velocity field is ~ 10 Mpc (Tselikhovich & Hirata 2010), which is much larger than the typical separation between atomic-cooling halos of interest. Thus, the root-mean-square value of the streaming velocity can represent those at the locations of halos. Intriguingly, the number densities of massive pristine DM halos at $15 \lesssim z \lesssim 20$ are $\mathcal{N} \simeq 10^{-5} - 10^{-4} \text{ Mpc}^{-3}$ for $T_{\text{vir}} \sim 2 \times 10^4$ K, and $\mathcal{N} \simeq 10^{-8} - 10^{-6} \text{ Mpc}^{-3}$ for $T_{\text{vir}} \sim 4 \times 10^4$ K.

We further investigate the dependence of our results on the streaming velocity, focusing on DM halos with $M_0 = 4.7 \times 10^7 M_\odot$ and $z_0 = 15$ ($T_{\text{vir}} = 2 \times 10^4$ K). As shown in Figure 2(a) and Table 1, The probability of pristine halos increases (decrease) for higher (lower) v_{bsm} because the mass gap between M_{cool} and M_0 becomes smaller (larger). we obtain $\mathcal{P}_{Z=0} \simeq (4.0 \pm 2.8) \times 10^{-6}$ for $v_{\text{bsm}} = \sigma_{\text{bsm}}$ and $\mathcal{P}_{Z=0} = 8.9 \times 10^{-2}$ for $v_{\text{bsm}} = 3\sigma_{\text{bsm}}$. Combined with the volume fraction of the Universe with the streaming velocities ($f_{1\sigma} \simeq 0.4$ and $f_{3\sigma} \simeq 5.9 \times 10^{-6}$), the number density of DM halos of interest is estimated as $\mathcal{N} \simeq (2.6 \pm 1.5) \times 10^{-6} \text{ Mpc}^{-3}$ for $v_{\text{bsm}} = \sigma_{\text{bsm}}$ and $\mathcal{N} \simeq 8.0 \times 10^{-7} \text{ Mpc}^{-3}$ for $v_{\text{bsm}} = 3\sigma_{\text{bsm}}$, respectively (see Figure 2b). As a result, we find that the number density can be maximized at $v_{\text{bsm}} \simeq 2\sigma_{\text{bsm}}$. Therefore, we adopt $v_{\text{bsm}} = 2\sigma_{\text{bsm}}$ as our fiducial case in the following sections.

Compared to previous work with cosmological simula-

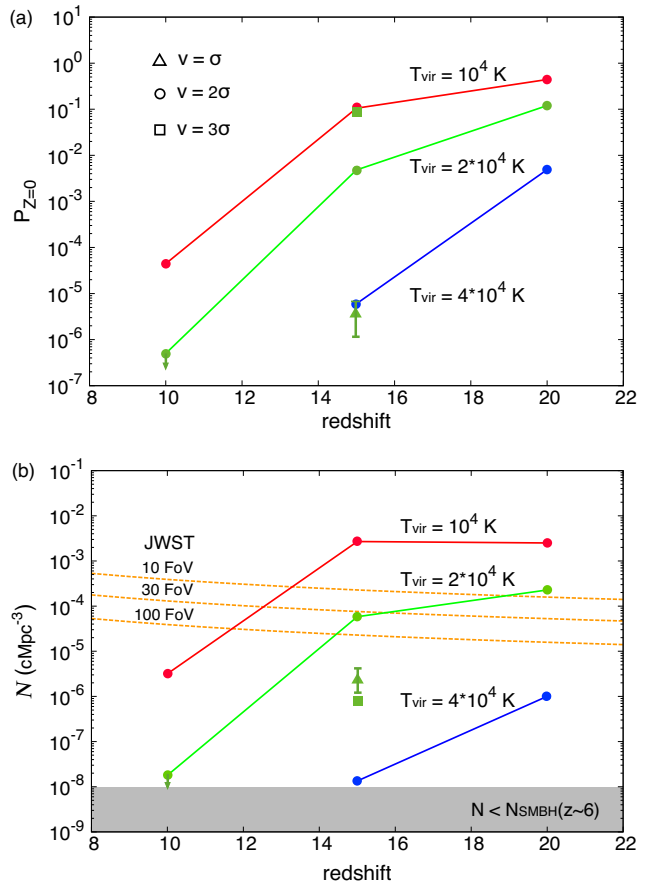


Figure 2. (a) Redshift-evolution of the probability for a DM halo to remain pristine as a result of suppressing star formation due to strong BSM with $v_{\text{bsm}} = 2\sigma_{\text{bsm}}$ (circle) and violent megers of gaseous halos caused by the BSM. Each line corresponds to the case with $T_{\text{vir}} \simeq 10^4$ K (red), 2×10^4 K (green), and 4×10^4 K (blue). The probability decreases for more massive halos at lower redshift because the mass differences with the minimum cooling mass become larger (see the green and blue regions in Fig. 1). The dependence on streaming velocities is shown for $T_{\text{vir}} = 2 \times 10^4$ K at $z = 15$: $v_{\text{bsm}}/\sigma_{\text{bsm}} = 1$ (triangle) and 3 (square). For each of these halos, we have many realizations of its merger trees so that the statistical errors become smaller than 0.1 $\mathcal{P}_{Z=0}$ (except for a case with $v_{\text{bsm}} = \sigma_{\text{bsm}}$). (b) The number density of massive pristine DM halos as a function of redshift. Orange curves show the minimum number densities required for a PopIII galaxy to be detected by JWST, assuming a duty cycle of PopIII galaxies (see Eq. 26), within three different fields of view $\Delta\Omega_{\text{obs}} = 10, 30$ and 100 FoV from the top to bottom, where FoV = 9.7 arcmin 2 . In the gray region, the number density is lower than that of high- z SMBHs ($\sim 1 - 10 \text{ Gpc}^{-3}$).

tions, we can justify our choice of $C (= 1.5)$. Schauer et al. (2017) have found 36 DM halos with $M_{\text{vir}} \gtrsim 3 \times 10^7 M_\odot$ at $z = 15$, where gas has just collapsed, in a rare patch of the Universe with $v_{\text{bsm}} = 3\sigma_{\text{bsm}}$. Since the volume of their simulation is $(4h^{-1} \text{ cMpc})^3$, the number density of massive DM halos containing pristine gas is $\sim 1.1 \times 10^{-6} \text{ cMpc}^{-3}$ at $z = 15$, which is consistent with our result for $C = 1.5$ ($\mathcal{N} \simeq 8.0 \times 10^{-7} \text{ Mpc}^{-3}$) or rather implies $C \gtrsim 1.5$.

It is also worth estimating the lower bound of the probability by assuming $C = 1$, which corresponds to the pressure-free collapse. For $v_{\text{bsm}} \simeq 2\sigma_{\text{bsm}}$, we obtain $\mathcal{P}_{Z=0} \sim 5.7 \times 10^{-5}$

for DM halos with $M_0 = 4.7 \times 10^7 M_\odot$ at $z_0 = 15$. Then, this probability ~ 80 times smaller than that for $C = 1.5$, and the number density of DM halos of interest is $\sim 7.0 \times 10^{-7} \text{ cMpc}^{-3}$.

The probability for a DM halo to remain pristine depends on the critical mass fraction f_{cr} , above which the merger events can suppress star formation temporarily ($f_{\text{cr}} = 1/4$ is our fiducial value). The results are summarized in Table 2. The fraction of DM halos where the gas remains pristine decreases with f_{cr} and is fitted by $\mathcal{P}_{Z=0} = \exp(-Af_{\text{cr}} + B)$, where $A = 23.85$ and $B = 0.64$. For $f_{\text{cr}} \lesssim 0.3$, the fraction is sufficiently high for the detection of such objects by JWST (see §3.3). In order to quantify the critical mass ratio for quenching star formation due to halo mergers, hydrodynamical simulations are necessary, which we leave to future work.

3 FORMATION OF MASSIVE SEED BHS AND POPULATION III GALAXIES

3.1 Cold accretion streams

In a rare region of the high- z Universe, where strong BSM significantly suppresses star formation as discussed in §2, the gas can be kept primordial even in a massive DM halo with $T_{\text{vir}} \gtrsim 10^4 \text{ K}$. The inflow rate of the pristine gas from larger scales is estimated as

$$\dot{M}_{\text{gas}} \simeq f_b \frac{V_{\text{vir}}^3}{G} \simeq 6.6 \times 10^{-2} T_{\text{vir},4}^{3/2} M_\odot \text{ yr}^{-1}, \quad (13)$$

(e.g., White & Frenk 1991; Mayer et al. 2015), where the baryon fraction, $f_b \equiv \Omega_b/\Omega_m$ is set to 0.16. A significant fraction of the gas can accrete onto the galactic center through cold streams. We define the gas accretion rate along one stream as $\dot{M}_s = \epsilon_s \dot{M}_{\text{gas}}$, where the fraction of $\epsilon_s (< 1)$ is given by $1/(\text{number of streams})$ and is set to $\epsilon_s \simeq 0.3$ as our fiducial value.

According to cosmological simulations of galaxy formation, the typical stream width inside the halo is a few percent of the virial radius (Kereš et al. 2005; Ocvirk et al. 2008; Dekel et al. 2009a; Ceverino et al. 2010). The cold accretion flow becomes denser at smaller radii because of contraction in the DM gravitational potential. As a result of this, the geometry of the flow seems a conical one rather than cylindrical one. Assuming a conical stream with an opening angle of θ_s , a half of the stream width is given by $R_s \simeq r\theta_s/2 = 0.1r(\theta_s/0.2)$, where r is the distance from the center of the halo. Such narrow cold streams with supersonic velocities penetrate well inside the virial radius, supplying gas and angular momentum towards the nuclear galactic disc. In the interface region between the streams and disc, the gas dynamics is governed by a combination of hydrodynamical, thermal and gravitational instabilities, shocks in the streams, and interactions of streams with other streams and/or the inner disc (e.g., Dekel et al. 2009b; Ceverino et al. 2010). Danovich et al. (2015) have investigated the nature of cold-stream penetration inside massive galaxies with $M_{\text{vir}} \simeq 10^{11} - 10^{12} M_\odot$ at $1 < z < 4$. They found that while most cold streams coherently join the rotationally supported central disc, a significant fraction ($\sim 30\%$) of the cold gas has a counter-rotation component with respect to the total angular momentum. In other words, for an atomic

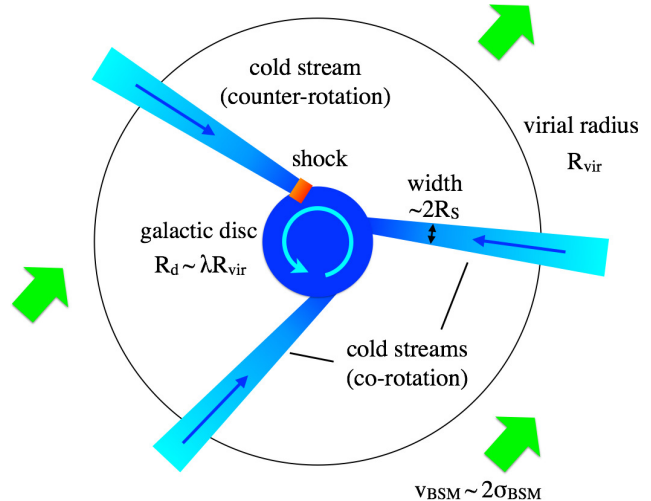


Figure 3. A schematic picture of a massive DM halo fed by cold streams along large-scale DM filaments in a rare patch of the Universe with a high streaming velocity of $v_{\text{bsm}} = 2\sigma_{\text{bsm}}$. The cold streams with a half width of R_s penetrate inside the virial radius of R_{vir} to the vicinity of the central galactic disc with a radius of $R_d \simeq \lambda R_{\text{vir}}$. Cold streams co-rotating with the host galaxy feed the central disc smoothly and lead to active star formation of ordinary PopIII stars. On other hand, the counter-rotating cold stream collides with the disc and/or other streams, forming strong shocks. If the shocked gas is hot and dense enough to dissociate H_2 (see Eqs. 17 and 20), a massive self-gravitating cloud forms at the interface and collapse directly into a massive seed BH.

cooling halo fed by three cold streams (i.e., $\epsilon_s \simeq 0.3$), one of them settles onto the central disc with experiencing strong shocks (see §3.2), but the other two smoothly supply gas to the disc (see §3.3).

The size of the galactic disc is characterized by the DM spin parameter of λ_{dm} as

$$R_d = \lambda_{\text{dm}} R_{\text{vir}}, \quad (14)$$

(Fall & Efstathiou 1980; Mo et al. 1998). Here, we assume that the angular momentum of cold streams is the same as that of DM halos. Danovich et al. (2015) have pointed out that for massive galaxies at $1 < z < 4$, the elongated streams gain angular momentum by tidal torques more than the DM halos, in fact, $\lambda_{\text{gas}} \sim (2-3)\lambda_{\text{dm}}$ at $r \gtrsim R_{\text{vir}}$. Thus, cold streams with a higher angular momentum dissipate at a relatively large radius of $\sim 0.3(\lambda_{\text{dm}}/0.15) R_{\text{vir}}$. However, this effect becomes less important for high-redshift galaxies (see their figure 7), which is consistent with the spin properties of mini-halos at $10 < z < 25$, where the mean spin parameters are estimated as $\lambda_{\text{gas}} = 0.0498$ and $\lambda_{\text{dm}} = 0.0495$ (Hirano et al. 2014). Therefore, we assume $\lambda_{\text{gas}} \simeq \lambda_{\text{dm}} (\equiv \lambda)$ and adopt $\lambda = 0.05$ as our fiducial model.

The inflow velocity of the cold stream does not follow the corresponding free-fall profiles. Instead, the velocity can be approximated as $v_{\text{in}} \simeq V_{\text{vir}}$, independent of the distance from the center of the halo (Goerdt & Ceverino 2015). In fact, several cosmological simulations for atomic-cooling halos suggest that the inflow velocity is $\sim 15-20 \text{ km s}^{-1}$ inside the virial radii (Greif et al. 2008; Wise et al. 2008) and near the edge of the central disc (Schauer et al. 2017). The ve-

locity is as high as the circular velocity, i.e., $v_{\text{in}} = \epsilon_v V_{\text{vir}}$. We set $\epsilon_v = 1.5$ as our fiducial value. Assuming steady accretion, we can estimate the gas density of a cone-like cold stream at the outer edge of the disc ($r = R_d$) as

$$\begin{aligned} \rho &= \frac{4\dot{M}_s}{\pi v_{\text{in}} (\theta_s R_d)^2}, \\ &\simeq 3.7 \times 10^{-21} \hat{\lambda}^{-2} \hat{\theta}_s^{-2} \left(\frac{1+z}{16} \right)^3 \text{ g cm}^{-3}, \end{aligned} \quad (15)$$

where $\hat{\lambda} = \lambda/0.05$ and $\hat{\theta}_s = \theta_s/0.2$.

The gas density inside the central gaseous disc is high enough to form H_2 molecules in the absence of strong shocks. A large amount of pristine gas with \sim a few $\times 10^6 M_\odot$ (see Eq. 22) forms ordinary PopIII stars with $M_\star \sim 10 - 100 M_\odot$ and evolve to a massive PopIII galaxy. On the other hand, if cold streams with counter-rotation components dissipate due to shocks, H_2 is dissociated efficiently depending on the post-shock density and form an SMS with $\sim 10^5 M_\odot$, which eventually collapses into a massive seed BH. In the following sections of §3.2 and 3.3, we discuss the subsequent evolution pathways in the two distinct cases.

3.2 Massive seed BH formation via colliding cold streams with the central disc

A cold stream with a counter-rotation component with respect to the total angular momentum is likely to collide with the outer edge of the galactic gaseous disc and/or other streams near the disc. The temperature of the cold stream is as low as $T \lesssim 8000$ K due to Ly α cooling and H_2 cooling. Since the sound speed is estimated as $c_s \simeq 2.6 \text{ km s}^{-1} (T/10^3 \text{ K})^{1/2}$, the Mach number is as high as $v_{\text{in}}/c_s \sim 4.6\epsilon_v (T_{\text{vir}}/10T)^{1/2}$. In such a strong shock limit, the gas density is enhanced by a factor of four, i.e., $\rho_{\text{post}} \simeq 4\rho$ behind the shock front at $r \simeq R_d$,

$$n_{\text{post}} \simeq 1.4 \times 10^4 \hat{\lambda}^{-2} \hat{\theta}_s^{-2} \left(\frac{1+z}{16} \right)^3 \text{ cm}^{-3}, \quad (16)$$

where the mean molecular weight of the postshock gas is set to 0.64 (fully ionized hydrogen and neutral helium). The post-shock temperature is estimated as

$$T_{\text{post}} \simeq \frac{3\mu m_p}{16k_B} v_{\text{in}}^2 \simeq 8.4 \times 10^3 T_{\text{vir},4} \text{ K}. \quad (17)$$

We describe the necessary conditions for suppressing H_2 formation via collisional dissociation in dense and hot shocked gas. Inayoshi & Omukai (2012) have studied thermal evolution of the shocked gas including chemical reactions among primordial species, and found that once the shocked gas enters a dense and hot region satisfying

$$T_{\text{post}} > 5.2 \times 10^3 \text{ K} \left(\frac{n_{\text{post}}}{10^4 \text{ cm}^{-3}} \right)^{-1}, \quad (18)$$

the shocked gas never cools down via H_2 cooling because of H_2 collisional dissociation. This condition can be rewritten in terms of the DM halo properties as

$$T_{\text{vir},4} > 0.44 \hat{\lambda}^2 \hat{\theta}_s^2 \left(\frac{1+z}{16} \right)^{-3}. \quad (19)$$

In addition, we require more massive haloes (i.e., higher virial temperature) to realize deep penetration of cold

streams due to efficient radiative cooling. Although the critical virial temperature is still uncertain, we conservatively assume the critical value to be $T_{\text{vir}} = 2 \times 10^4$ K, making cooling timescale shorter. Therefore, the necessary conditions for SMS formation are given by

$$T_{\text{vir},4} \gtrsim \max \left[0.44 \hat{\lambda}^2 \hat{\theta}_s^2 \left(\frac{1+z}{16} \right)^{-3}, 2.0 \right], \quad (20)$$

which is shown in Fig. 1 (the hatched green region). We note that the boundary of the H_2 -dissociation dominant region is almost independent of the electron (x_e) and H_2 fraction (x_{H_2}) in the pre-shock gas, as long as $x_e \gtrsim 10^{-4}$ and $x_{\text{H}_2} \lesssim 10^{-3}$ (see Figure 2 in Inayoshi & Omukai 2012). However, the location of the boundary shifts to higher densities due to metal-line cooling for $Z \gtrsim 10^{-3} Z_\odot$ (see Figure 3 in Inayoshi & Omukai 2012).

Behind the shock front, the gas never cools below $T < 8000$ K because of the lack of H_2 . The shocked gas is accumulated and contract isobarically with the same ram pressure from the shock front, where $P_{\text{ext}} \simeq \rho v_{\text{in}}^2$. An isothermal cloud embedded in an external pressure P_{ext} cannot exist in stable equilibrium if the mass of the cloud exceeds a critical value (e.g., Ebert 1955; Bonnor 1956):

$$\begin{aligned} M_{\text{BE}} &\simeq 1.05 \frac{\theta_s \lambda}{\sqrt{\epsilon_s \epsilon_v f_b}} \left(\frac{c_s}{V_{\text{vir}}} \right)^4 M_{\text{vir}}, \\ &\simeq 9.6 \times 10^4 \hat{\lambda} \hat{\theta}_s T_{\text{vir},4}^{-1/2} \left(\frac{1+z}{16} \right)^{-3/2} M_\odot. \end{aligned} \quad (21)$$

For our fiducial case, the shocked gas layer becomes massive enough to be unstable against its self-gravity in a timescale of $M_{\text{BE}}/\dot{M}_s \sim 1.1 \text{ Myr} (T_{\text{vir},4}/2)^{-2}$. Since this timescale is sufficiently shorter than typical lifetime of massive stars, the SMS forming cloud would not be enriched by metals produced by supernovae, which would happen in the central disc at $t \gtrsim 4 - 10 \text{ Myr}$ (see discussions in §3.3). After the onset of the gravitational instability, the gas cloud collapse in a runaway fashion (e.g., Larson 1969) and form a single protostar without major episodes of fragmentation (e.g., Regan et al. 2014; Inayoshi et al. 2014; Becerra et al. 2015; Latif et al. 2016a). The protostar grows via rapid accretion from the massive clump at a rate of $\dot{M}_\star \simeq 20 c_s^3/G \simeq 2 M_\odot \text{ yr}^{-1}$ (e.g., Inayoshi et al. 2014).

3.3 Massive PopIII galaxies formation via rapid feeding of pristine gas

Next, let us consider the properties of a galaxy formed by metal-free gas at the center of the most massive DM halo with $M_{\text{vir}} \gtrsim 5 \times 10^7 M_\odot$ ($T_{\text{vir}} \gtrsim 2 \times 10^4$ K at $z \gtrsim 15$). Assuming that the mean gas density at $r \lesssim R_d$ is given by Eq. (15), the disc mass is estimated as

$$M_d \simeq 0.085 \hat{\lambda} \hat{\theta}_s \sqrt{\frac{T}{T_{\text{vir}}}} M_{\text{vir}}. \quad (22)$$

For $T = 8000$ K and $T_{\text{vir}} = 2 \times 10^4$ K, we obtain $M_d \simeq 0.054 \hat{\lambda} M_{\text{vir}} \simeq 0.34 \hat{\lambda} (\Omega_b/\Omega_m) M_{\text{vir}}$. Therefore, we find that $M_d \simeq 2.7 \times 10^6 \hat{\lambda} M_\odot$ of gas is concentrated to the nuclear disc. Note that the disc mass is consistent with that of a disc formed in a massive halo with $M_{\text{vir}} \simeq 10^8 M_\odot$ at $z \simeq 15$ estimated with cosmological simulations without radiative feedback (Pawlik et al. 2011). The gas-rich disc becomes unsta-

ble due to the self-gravity, exciting bar modes to transport angular momentum and/or fragmenting to clumps. The instability is characterized in terms of the Toomre's parameter Q , evaluated at $r = R_d$ as

$$Q = \frac{c_s \kappa}{\pi G \Sigma_d} \simeq 0.63 \hat{\theta}_s^{1/2} \left(\frac{T}{T_{\text{vir}}} \right)^{1/4}, \quad (23)$$

where Σ_d is the surface density of the disc, and κ is the epicyclic frequency, which is related to the orbital frequency Ω as $\kappa^2 = r d\Omega^2/dr + 4\Omega^2$. We here adopt $\kappa = \Omega$ for Keplerian orbits. Note that for $T = 8000$ K and $T_{\text{vir}} = 2 \times 10^4$ K, we obtain $Q \simeq 0.5$ (< 1), for which fragmentation and star formation are triggered. The gas density of each fragment is as high as $n \sim 10^3 \text{ cm}^{-3}$ and thus the free-fall timescale of ~ 1 Myr is significantly shorter than the lifetime of $\sim 4 - 10$ Myr for massive PopIII stars with $M_* \simeq 10 - 50 M_\odot$ (e.g., [Marigo et al. 2001](#)). In the following, we consider the early stage of star formation within ~ 3 Myr because (1) supernova feedback can be neglected and (2) the detectability of younger PopIII galaxies by JWST is higher.

The absence of supernova feedback in the early stage ($t \lesssim 3$ Myr) enables a high star formation efficiency $\epsilon_* \equiv M_{*,\text{tot}}/M_d$, where $M_{*,\text{tot}}$ is the total mass of PopIII stars formed in the disc. For massive PopIII stars, ionizing radiation emitted from accreting protostars heats the ambient gas and photo-evaporates their parent cloud ([McKee & Tan 2008](#); [Hosokawa et al. 2011](#)). [Hirano et al. \(2014\)](#) suggest that the properties of parent clouds, namely accretion rates onto protostars, determine the star formation efficiency and the initial mass function (IMF) of stars. In fact, the efficiency is estimated as $\epsilon_* \simeq 0.3$ for $10 \lesssim M_*/M_\odot \lesssim 10^2$ (IMFa), and $\epsilon_* \simeq 0.5$ for $10^2 \lesssim M_*/M_\odot \lesssim 10^3$ (IMFb). Thus, the total stellar mass is estimated as

$$M_{*,\text{tot}} \simeq \begin{cases} 8 \times 10^5 \lambda M_\odot & (\text{IMFa}), \\ 1.4 \times 10^6 \lambda M_\odot & (\text{IMFb}). \end{cases} \quad (24)$$

We note that the star-formation efficiencies we assumed would be an upper limit because ionizing radiation from newly-born stars could affect nearby star forming clouds and reduce the total star formation efficiency in the galaxy. With a spectral synthesis model for PopIII stars, [Zackrisson et al. \(2011\)](#) discussed the detectability of PopIII galaxies through broadband imaging at 10σ after a 100 hr exposure with JWST. In the early stage of a star-burst episode within ~ 3 Myr, the minimum mass of PopIII galaxies required for the detection is estimated as

$$M_{*,\text{tot}}^{\text{obs}} \simeq \begin{cases} (4 - 10) \times 10^5 M_\odot & (\text{IMFa}), \\ (2 - 3) \times 10^5 M_\odot & (\text{IMFb}), \end{cases} \quad (25)$$

where the lower (higher) value corresponds to that at $z = 10$ (15). The exposure time for the detection is $t_{\text{exp}} \simeq (6.3 - 40) \times (\lambda/0.1)^{-2}$ hr for IMFa, but is only $t_{\text{exp}} \simeq (0.5 - 1.1) \times (\lambda/0.1)^{-2}$ hr for IMFb. Although the exposure time is shorter for higher spin, the free-fall timescale in the disc is comparable or longer than the lifetime of massive PopIII stars. Therefore, our assumption neglecting the effects of supernova explosions breaks down for $\lambda \gtrsim 0.2$. In addition, the conditions for massive seed BHs becomes more severe for $\lambda \gtrsim 0.2$ because the post-shock density is not high enough to dissociate H_2 . Overall, we find that $\lambda = 0.1$ and very top-heavy IMF (IMFb) are an interesting combination

in terms of massive seed BH formation and the detectability of PopIII galaxies with JWST.

We aim to detect massive PopIII galaxies at $10 \lesssim z \lesssim 15$. For this redshift range, Ly α and HeII 1640 Å emission can be observed by NIRCcam of JWST (e.g., [Tumlinson & Shull 2000](#); [Oh et al. 2001](#)). As discussed in [Zackrisson et al. \(2011\)](#), we could identify young PopIII galaxies with the ages of $t_{\text{burst}} \simeq 3$ Myr, using the JWST color criteria (see also [Inoue 2011](#)). Thus, considering the duty cycle of PopIII star bursts, we can estimate the effective comoving volume where PopIII galaxies are detected as

$$\begin{aligned} \Delta V_{\text{obs}}(z) &= \Delta \Omega_{\text{obs}} \frac{dV_c}{dz} \frac{dz}{dt_r} t_{\text{burst}}, \\ &\simeq 4.4 \times 10^3 \text{ cMpc}^3 \left(\frac{t_{\text{burst}}}{3 \text{ Myr}} \right) \left(\frac{1+z}{16} \right)^\gamma \left(\frac{\Delta \Omega_{\text{obs}}}{10 \text{ FoV}} \right), \end{aligned} \quad (26)$$

where V_c is the comoving volume, t_r is the time in a source's cosmic rest frame, $\Delta \Omega_{\text{obs}}$ is the observed field of view (one FoV $\simeq 9.7 \text{ arcmin}^2$), and $\gamma \simeq 1.406$ at $10 \leq z \leq 20$. In Fig. 2 (b), we show the number density of PopIII galaxies required for the detection in a given total FoVs is $\simeq 1/\Delta V_{\text{obs}}(z) \simeq 2.3 \times 10^{-4} \text{ cMpc}^{-3} [(1+z)/16]^{-\gamma} (\Delta \Omega_{\text{obs}}/10 \text{ FoV})^{-1}$. The threshold value is comparable to the number density of PopIII galaxies ($n \sim 10^{-4} \text{ cMpc}^{-3}$) with $T_{\text{vir}} \simeq 2 \times 10^4$ K. In order to detect one PopIII galaxy by JWST, we require $\simeq 1$ hr observations in different $\simeq 30$ areas, i.e., the total field of view $\sim 300 \text{ arcmin}^2 \sim 0.1 \text{ deg}^2$. This total area corresponds to $\lesssim 3$ % of Ultra deep field of Subaru Hyper Suprime Cam ([Aihara et al. 2018](#))⁵.

4 DISCUSSION

4.1 Implications of subsequent BH evolution

Once a seed BH with a mass of $M_\bullet \sim 10^5 M_\odot$ forms in a massive DM halo with $M_{\text{vir}} \sim 10^8 M_\odot$, subsequent growth via gas accretion and/or BH mergers is required to reach $M_\bullet \sim 10^9 M_\odot$ by $z \simeq 6 - 7$ (e.g., [Tanaka & Haiman 2009](#); [Valiante et al. 2016](#); [Pezzulli et al. 2016](#)). Assuming the Eddington-limited accretion, the BH growth timescale from 10^5 to $10^9 M_\odot$ is estimated as $\simeq 0.46$ Gyr, where the radiative efficiency is set to a constant value of $\eta = 0.1$. The growth time is marginally shorter than the cosmic time from $z = 20$ to 7 ($\simeq 0.57$ Gyr) ([Haiman & Loeb 2001](#)).

[Valiante et al. \(2016\)](#) have investigated the relative role of light seeds (i.e., PopIII remnant BHs) and heavy (massive) seeds as BH progenitors of the first SMBHs, conducting semi-analytical calculations. They concluded that, as long as gas accretion is assumed to be Eddington-limited, heavy BH seeds at $z \gtrsim 15$ are required to form SMBHs with $\gtrsim 10^9 M_\odot$ by $z \simeq 6$. Moreover, in their models, only ~ 13 % of the total amount of seeds formed in protogalaxies can be SMBH progenitors, because most seeds follow minor branches of the merger tree and is in satellite galaxies. Therefore, the number density we estimated in Eq. (12) could be reduced by one order of magnitude. It is worth discussing the occupation fraction of seed BHs in DM halos under streaming velocities (see also [Tanaka & Li 2014](#)).

Super-Eddington accretion is an alternative way to form

⁵ <https://hsc-release.mtk.nao.ac.jp/doc/>

high- z SMBHs with $\gtrsim 10^9 M_\odot$. In a massive halo forming a massive seed BH with $M_\bullet \sim 10^5 M_\odot$, the gas density as high as $\gtrsim 10^4 \text{ cm}^{-3} [(1+z)/16]^3$. In this case, since an HII region formed by ionizing radiation due to the accreting BH is confined within the Bondi radius of the BH (i.e., $R_{\text{HII}} < R_{\text{Bondi}}$), a steady accretion at $\gtrsim 300 \dot{M}_{\text{Edd}}$ can be realized (Inayoshi, Haiman & Ostriker 2016; Sakurai, Inayoshi & Haiman 2016b; see also Volonteri & Rees 2005; Alexander & Natarajan 2014; Madau et al. 2014; Pacucci & Ferrara 2015; Sugimura et al. 2017, 2018; Takeo et al. 2018)⁶, where $\dot{M}_{\text{Edd}} \equiv 16 L_{\text{Edd}}/c^2$. A semi-analytical model by Pezzulli et al. (2016) also supports that hyper-Eddington accretion at $\gtrsim 300 \dot{M}_{\text{Edd}}$ would likely occur at $10 \lesssim z \lesssim 25$. Moreover, a sufficient amount of gas supply through intense cold streams would feed the BH (e.g., Di Matteo et al. 2012). The further study of super(hyper)-Eddington accretion of BHs in more realistic situations will be left in future work.

We discuss the early stage of massive DM halos hosting seed BHs and PopIII galaxies. The relation between BHs and galaxies is quite important to understand their coevolution over the cosmic history (Kormendy & Ho 2013). From Eqs. (21) and (22), we can estimate the mass ratio of seed BHs to PopIII galaxies as $M_\bullet/M_{\star, \text{tot}} \sim 0.4 \epsilon_\star^{-1} (T/T_{\text{vir}})^{3/2}$, independent of θ_s and λ . Since violent mergers of atomic-cooling halos associated with strong BSM can keep the gas pristine in halos with $T_{\text{vir}} \lesssim 4 \times 10^4 \text{ K}$, the mass ratio is estimated as $\sim 0.04 \epsilon_\star^{-1}$. The mass ratio is $\gtrsim 20$ times higher than the SMBH-bulge mass ratio observed in the local Universe, $M_\bullet/M_{\text{bulge}} \simeq 5 \times 10^{-3} (M_{\text{bulge}}/10^{11} M_\odot)^{0.16}$ (e.g., Magorrian et al. 1998; Gültekin et al. 2009; Kormendy & Ho 2013). On the other hand, Atacama Large Millimeter/submillimeter Array (ALMA) observations of quasar host galaxies at $z \sim 6$ implies that the mass ratios between the SMBHs and the gas dynamical mass are an order of magnitude higher than the mean value found in local Universe (Wang et al. 2013, 2016). These observational results suggest that SMBHs in high- z quasars remain overmassive. To explore the SMBH-galaxy coevolution, we need an observational program with multi-frequencies including near-infrared radiation with JWST and X-rays with a future satellite, e.g., Lynx⁷.

4.2 Caveats

4.2.1 Star formation in cold streams

Self-gravitating cold streams potentially lead to star formation (Nakamura & Umemura 2001, 2002), preventing shock formation at the edge of the central galactic disc. In a protogalaxy, the typical line mass density of cold streams is given by $m_{\text{line}} \equiv \pi \rho R_s^2 = 1.1 \times 10^4 T_{\text{vir},4} [(\epsilon_s/\epsilon_v)/0.2] M_\odot \text{ pc}^{-1}$. For a cylindrical filament in a hydro-static equilibrium, the stability analysis provides a critical line mass density of $m_{\text{crit}} = 2c_{\text{eff}}^2/G$, above which the filament starts to collapse and fragment due to its self-gravity (Ostriker 1964). The effective sound speed is given by $c_{\text{eff}}^2 = c_s^2 + \sigma_{\text{turb}}^2$, where σ_{turb} is the turbulent velocity. One possible origin of the turbulent

velocity is BSM⁸. The typical velocity is roughly estimated as $\sigma_{\text{turb}} \simeq \sqrt{(v_{\text{cool}}^2 - v_0^2)}$ or

$$\sigma_{\text{turb}} \simeq 3.5 \text{ km s}^{-1} \left(\frac{v_{\text{bsm}}}{2\sigma_{\text{bsm}}} \right) \left(\frac{1+z}{16} \right), \quad (27)$$

and thus the critical line mass density is

$$m_{\text{crit}} \simeq 5.6 \times 10^3 M_\odot \text{ pc}^{-1} \times \left[0.56 \left(\frac{T}{10^3 \text{ K}} \right) + \left(\frac{v_{\text{bsm}}}{2\sigma_{\text{bsm}}} \right)^2 \left(\frac{1+z}{16} \right)^2 \right]. \quad (28)$$

For $v_{\text{bsm}} = 2\sigma_{\text{bsm}}$, we obtain $m_{\text{crit}} \simeq 8.7 \times 10^3 (1.3 \times 10^4) M_\odot \text{ pc}^{-1}$ at $z = 15(20)$. Since the line mass density is marginally higher than the critical value, the cold stream could be unstable against its self-gravity. However, we note that this argument is valid for a filamentary stream in hydrostatic equilibrium. In reality, since a cold stream we consider has a bulk inward supersonic velocity, fragmentation would be less efficient than that from a static equilibrium configuration. Even if the gas filament began to contract and fragment into smaller clumps, the collapse would proceed in a timescale of $t_{\text{col}} = C'/\sqrt{4\pi G \bar{\rho}}$, where $C' \simeq 3$ for the most unstable mode against fragmentation when $m_{\text{line}}/m_{\text{crit}} \sim 1 - 2$. Thus, we obtain the ratio of t_{col} to the infall timescale of the cold stream $t_{\text{inf}} (\equiv r/v_{\text{in}})$ as

$$\frac{t_{\text{col}}}{t_{\text{inf}}} = \frac{C'}{2} \sqrt{\frac{\epsilon_\star^3}{\epsilon_s f_b}} \sim 13 \left(\frac{C'}{3} \right) \left(\frac{\epsilon_s}{0.3} \right)^{-1/2} \left(\frac{\epsilon_v}{1.5} \right)^{3/2}. \quad (29)$$

Therefore, we find that the cold stream is unstable against its self-gravity, but is likely to accrete onto the central region before fragmenting and forming stars. Note that the ratio of $m_{\text{line}}/m_{\text{crit}}$ and Eq. (29) do not depend on the choice of λ .

Recently, Mandelker et al. (2017) have discussed formation of metal poor globular-clusters via massive clumps in cold accretion streams in protogalaxies with $M_{\text{halo}} \sim 10^{10} M_\odot$ at $z \sim 6$. We note that our scenario does not work in their situation because (1) the line mass density tends to be higher in a massive halo and (2) the critical line mass density becomes smaller at lower redshifts ($z < 10$) due to the decay of the BSM. Applying the above argument to a massive halo with $M_{\text{halo}} \sim 10^{10} M_\odot$ at $z \sim 6$, we obtain $m_{\text{line}}/m_{\text{crit}} \gtrsim 10$. Since such a massive stream has a higher concentration of the initial density and $C' \lesssim 1$, the collapse timescale could be comparable or shorter than the infall timescales.

4.2.2 Shock structure in cold streams

In this paper, we discuss the properties of cold accretion flows penetrating deeply inside a massive DM halo down to the nuclear disc. This would be plausible as long as the radiative cooling timescale is shorter than the dynamical timescale in the flow, $t_{\text{cool}} < t_{\text{dyn}}$. The critical conditions for the deep penetration would be given by $M_{\text{vir}} \lesssim 10^{12} M_\odot$ for lower-redshift massive halos (e.g., Birnboim & Dekel 2003; Dekel & Birnboim 2006). However, the critical conditions in

⁶ In this paper, the Eddington accretion rate is defined as $\dot{M}_{\text{Edd}} \equiv L_{\text{Edd}}/c^2$, and a high accretion rate of $\gtrsim 5000 \dot{M}_{\text{Edd}}$ from the Bondi radius is required for hyper-Eddington accretion.

⁷ <https://wwwastro.msfc.nasa.gov/lynx/>

⁸ Another possible origin of the turbulence would be gas accretion onto cold streams from the host halo (e.g., Klessen & Hennebelle 2010; Heitsch 2013). The typical turbulent velocity would be at most $\sim 1 \text{ km s}^{-1}$ in our fiducial case.

the low mass end are still uncertain. Here, we assume that deep penetration of cold streams occurs in DM halos with $T_{\text{vir}} \geq 2 \times 10^4$ K in order to ensure $t_{\text{cool}} < t_{\text{dyn}}$. In fact, [Fernandez et al. \(2014\)](#) found a certain level of penetration even in halos with $T_{\text{vir}} \simeq 10^4$ K when H_2 cooling is turned off and $\text{Ly}\alpha$ cooling carries energy away quickly. This result supports that what matters is not the gas temperature but the cooling timescale. They also studied the gas in DM haloes with $T_{\text{vir}} \lesssim 10^4$ K considering H_2 cooling, which is less efficient than $\text{Ly}\alpha$ cooling. In this case, cold gas accretes into the halo, but undergoes a series of weak shocks, reducing its infall velocity closer to the sound speed. As a result, the cold stream stalls before reaching the central region, and the shocked density is not high enough to dissociate H_2 . To explore the nature of cold streams in an atomic-cooling halo and to study the critical conditions for deep penetration to form dense shocks are left for future investigations.

For this purpose, we need to investigate a long-term evolution (\gtrsim a few Myr) of a galactic disc and cold streams, using some numerical techniques (sink particles and/or a minimum pressure floor) to save computation time. Simultaneously, we have to resolve a small scale of L to capture the physics of interaction between the disc and cold streams, and fragmentation of massive clumps at the edge of the disc. A plausible choice of the minimum spacial length for the simulations would be $L < \lambda_{\text{J}}/4 \sim 3$ pc, where λ_{J} is the Jeans length at $r \simeq R_{\text{d}}$ (see Appendix B, also [Truelove et al. 1997](#)).

4.2.3 Dynamical heating or gas collapse triggered by major mergers

In this paper, we assume that major mergers of DM halos disturb a dense gas core at the center and thus delay the onset of gravitational collapse of the cloud. However, one might expect that major mergers trigger the collapse instead. This issue has been studied by [Chon et al. \(2016\)](#) in a context of the SMS formation aided by strong LW radiation for suppressing H_2 . They found that frequent mergers of DM halos generally decrease the gas density at the core and prevent gravitational collapse via dynamical heating, which works more efficiently than that in ordinary PopIII star formation in low-mass DM halos with $\gtrsim 10^5 M_{\odot}$ (e.g., [Yoshida et al. 2003](#)). As discussed in §2, in this case the size of the gas core is smaller than the local Jeans length, and is unlikely to be unstable even after major mergers. In contrast, [Chon et al. \(2016\)](#) also found a case where gas collapse can be triggered by an *extremely frequent* major-merger event (six gaseous clumps merge in a short timescale; see their Figure 11). Through the event, the core mass is boosted by a factor of ~ 30 only within one dynamical timescale. Note that mass increase by a factor of $\gtrsim 10$ is required to induce the cloud collapse (see their Figure 19b). This situation seems much more extreme than those we consider in this paper, but similarly lead to the formation of massive DM halos containing pristine gas.

4.2.4 External metal enrichment

We note that external metal enrichment due to supernovae winds launched from DM halos in metal-polluted trees is negligible. With strong BSM ($v_{\text{bsm}} \gtrsim 2\sigma_{\text{bsm}}$), external enrichment could be caused by DM halos with $M_{\text{vir}} \gtrsim$

$M_{\text{cool}}(z) \simeq 2 \times 10^6 M_{\odot}$ at $15 < z < 25$. For such halo masses, we require energetic explosions by pair-instability supernovae (PISNe) to eject heavy elements into intergalactic media (IGM) and cause external metal enrichment ([Kitayama & Yoshida 2005](#); [Chiaki et al. 2018](#), see also [Smith et al. 2015](#); [Jeon et al. 2017](#)). Let us suppose that PISNe occur in the majority of DM halos with $M_{\text{vir}} \gtrsim M_{\text{cool}}$ at $z \simeq 20$. Since the number density of such halos is $n_{\text{h}} \simeq 10 \text{ cMpc}^{-3}$, an averaged distance between the PISN halos and pristine DM halos due to unusually frequent merger histories can be estimated as $d \simeq 320 \text{ ckpc}$ (comoving). [Greif et al. \(2007\)](#) have studied a similar situation that a $200 M_{\odot}$ PISN occurs in an even lower-mass halo with $M_{\text{vir}} \simeq 5 \times 10^5 M_{\odot}$ at $z = 20$ and enriches the IGM (see also [Wise & Abel 2008](#)). As a result, a metal-polluted bubble expands only to $\sim 32 \text{ ckpc}$ by $z \simeq 15$, which is much shorter than the typical distance between halos. Therefore, we can conclude that external metal enrichment of pristine DM halos is unlikely to occur in a region with $v_{\text{bsm}} \gtrsim 2\sigma_{\text{bsm}}$.

5 SUMMARY

We propose the formation of massive pristine dark-matter (DM) halos with masses of $\sim 10^8 M_{\odot}$, due to the dynamical effects by violent mergers in rare regions of the Universe with high baryonic streaming velocity relative to DM. Since the streaming motion prevents gas collapse into DM halos and delays prior star formation episodes, the gas remains metal-free until the halo reaches virial temperatures $\gtrsim 2 \times 10^4$ K. The minimum cooling mass of DM halos is boosted by a factor of $\sim 10 - 30$ because violent major mergers of gaseous halos further inhibit gas collapse. We use Monte Carlo merger trees to simulate the DM assembly history under a streaming velocity of twice the root-mean-square value, and estimate the number density of massive pristine DM halos as $\simeq 10^{-4} \text{ cMpc}^{-3}$. When the gas infall begins, efficient $\text{Ly}\alpha$ cooling drives cold streams penetrating inside the halo and feeding a central galactic disc. When one stream collides with the disc, strong shock forms dense and hot gas cloud, where the gas never forms due to effective H_2 dissociation. As a result, a massive gas cloud forms by gravitational instability and collapses directly into a massive black hole (BH) with $M_{\bullet} \sim 10^5 M_{\odot}$. Almost simultaneously, a galaxy with $M_{\star, \text{tot}} \sim 10^6 M_{\odot}$ composed of Population III stars forms in the nuclear region. If the typical stellar mass is as high as $\sim 100 M_{\odot}$, the galaxy could be detected with the *James Webb Space Telescope* even at $z \sim 15$. The BH would be fed by continuous gas accretion from the host galaxy, and grow to be a bright quasar such as those observed at $z \gtrsim 6$.

ACKNOWLEDGEMENTS

We thank Avishai Dekel, Shingo Hirano, Nir Mandelker, Greg Bryan, Micheal Norman, Takashi Hosokawa, Kohei Ichikawa, Eli Visbal and Chang-Goo Kim for useful discussions. This work is partially supported by the Simons Foundation through the Simons Society of Fellows (KI) and by NASA grant NNX15AB19G (ZH). ML thanks the support the Science Computing Core of Flatiron Institute.

APPENDIX A: MASS ACCRETION RATES THROUGH COLD FILAMENTS

We adopt Eq. (13) as gas accretion rates along cold streams. Here, we discuss a general function form of

$$\dot{M}_s \simeq \epsilon_s f_b A T_{\text{vir},4}^\alpha \left(\frac{1+z}{16} \right)^\beta. \quad (\text{A1})$$

Our fiducial case corresponds to $A = 0.41 M_\odot \text{ yr}^{-1}$, $\alpha = 3/2$, and $\beta = 0$. Alternatively, cosmological N-body simulations predict the mean accretion rate of total mass onto the virial radius of a massive halo with a mass of $10^{10} \lesssim M_{\text{vir}}/M_\odot \lesssim 10^{15}$ at a redshift of $0 \leq z < 15$ (Fakhouri et al. 2010) is well fit by $A = 0.16 M_\odot \text{ yr}^{-1}$, $\alpha = 1.65$, and $\beta = 0.85$. Note that the later formula might not be applicable for atomic-cooling halos. The accretion rate in Eq. (13) is higher than that in Eq. (A1) by a factor of 2.6 (2.0) at $z = 15$ (20) for $T_{\text{vir}} = 10^4 \text{ K}$.

APPENDIX B: PHYSICAL PROPERTIES OF GALACTIC DISCS

We here summarize the physical length and mass scales on galactic discs in massive DM halos with $T_{\text{vir}} \gtrsim 10^4 \text{ K}$. We adopt a simple model for the vertical structure of the disc, which has been used extensively and originally proposed by Spitzer (1942). In this model, where the gas distribution is assumed to be locally isothermal, the density profile is obtained as

$$\rho(r, z) = \rho_0 f(r) \text{sech}^2 \left(\frac{z}{2z_d} \right), \quad (\text{B1})$$

where $z_d = c_s / \sqrt{8\pi G \rho_0}$ and ρ_0 is the central density, which is set to the value in Eq. (15). For this gas profile in the disc, the surface density and the disc mass are estimated as $\Sigma_d = 4\rho_0 z_d f(r)$, and $M_d = 8\pi I \rho_0 z_d R_d^2$, where $I = \int f(r) r dr / R_d^2$. We obtain $I = 1$ for an exponential disc, $f(r) = \exp(-r/R_d)$, and $I = 1/2$ for a uniform disc mode, $f(r) = 1$ at $r \leq R_d$ and $f = 0$ at $r > R_d$. In Eq. (22), we obtain $M_d = 2\pi \rho_0 R_d^2 \times (2z_d)$, assuming $I = 1/2$ so that the scale height of the disc is given by $2z_d$,

$$H = \frac{2c_s}{V_{\text{vir}}} \sqrt{\frac{\epsilon_v}{32\epsilon_s f_b}} \theta_s R_d \simeq 0.4 \sqrt{\frac{T}{T_{\text{vir}}}} \hat{\theta}_s R_d, \quad (\text{B2})$$

where Eq. (15) is used. Using those equations, the Toomre's parameter is simply given by $Q \simeq \sqrt{H/R_d}$.

Finally, let us estimate the Jeans length of the post-shock gas, where a massive seed BH could form as discussed in §3.2. Since the gas density behind the shock front is $\gtrsim 4\rho_0$ due to compression by accreting gas and atomic-cooling at $T \gtrsim 8000 \text{ K}$, the Jeans length is as small as

$$\lambda_J \lesssim c_s \sqrt{\frac{\pi}{4G\rho_0}} \simeq 2H. \quad (\text{B3})$$

Thus, once dense gas is accumulated at the edge of the galactic disc, massive clumps can be unstable and collapse. Combined with Eq. (B2), for $T = 8000 \text{ K}$ and $T_{\text{vir}} = 2 \times 10^4 \text{ K}$, the Jeans length is estimated as

$$\lambda_J \lesssim 2.5 \times 10^{-2} \hat{\theta}_s \hat{\lambda} R_{\text{vir}} \simeq 13 \hat{\theta}_s \hat{\lambda} T_{\text{vir},4}^{1/2} \left(\frac{1+z}{16} \right)^{-3/2} \text{ pc}. \quad (\text{B4})$$

REFERENCES

- Agarwal B., Khochfar S., 2015, *MNRAS*, **446**, 160
 Aihara H., et al., 2018, *PASJ*, **70**, S4
 Aikawa Y., Herbst E., Roberts H., Caselli P., 2005, *ApJ*, **620**, 330
 Alexander T., Natarajan P., 2014, *Science*, **345**, 1330
 Bañados E., et al., 2018, *Nature*, **553**, 473
 Becerra F., Greif T. H., Springel V., Hernquist L. E., 2015, *MNRAS*, **446**, 2380
 Begelman M. C., Volonteri M., Rees M. J., 2006, *MNRAS*, **370**, 289
 Birnboim Y., Dekel A., 2003, *MNRAS*, **345**, 349
 Bonnor W. B., 1956, *MNRAS*, **116**, 351
 Bromm V., Loeb A., 2003, *ApJ*, **596**, 34
 Bryan G. L., Norman M. L., 1998, *ApJ*, **495**, 80
 Ceverino D., Dekel A., Bournaud F., 2010, *MNRAS*, **404**, 2151
 Chiaki G., Susa H., Hirano S., 2018, *MNRAS*, **475**, 4378
 Chon S., Hirano S., Hosokawa T., Yoshida N., 2016, *ApJ*, **832**, 134
 Chon S., Hosokawa T., Yoshida N., 2018, *MNRAS*, **475**, 4104
 Danovich M., Dekel A., Hahn O., Ceverino D., Primack J., 2015, *MNRAS*, **449**, 2087
 Dekel A., Birnboim Y., 2006, *MNRAS*, **368**, 2
 Dekel A., et al., 2009a, *Nature*, **457**, 451
 Dekel A., Sari R., Ceverino D., 2009b, *ApJ*, **703**, 785
 Di Matteo T., Khandai N., DeGraf C., Feng Y., Croft R. A. C., Lopez J., Springel V., 2012, *ApJ*, **745**, L29
 Ebert R., 1955, *Z. Astrophys.*, **37**, 217
 Eisenstein D. J., Loeb A., 1995, *ApJ*, **443**, 11
 Fakhouri O., Ma C.-P., Boylan-Kolchin M., 2010, *MNRAS*, **406**, 2267
 Fall S. M., Efstathiou G., 1980, *MNRAS*, **193**, 189
 Fan X., 2006, *New Astron. Rev.*, **50**, 665
 Fernandez R., Bryan G. L., Haiman Z., Li M., 2014, *MNRAS*, **439**, 3798
 Fialkov A., Barkana R., Tseliakhovich D., Hirata C. M., 2012, *MNRAS*, **424**, 1335
 Foster P. N., Chevalier R. A., 1993, *ApJ*, **416**, 303
 Glover S. C. O., 2016, preprint, ([arXiv:1610.05679](https://arxiv.org/abs/1610.05679))
 Goerd T., Ceverino D., 2015, *MNRAS*, **450**, 3359
 Greif T. H., Johnson J. L., Bromm V., Klessen R. S., 2007, *ApJ*, **670**, 1
 Greif T. H., Johnson J. L., Klessen R. S., Bromm V., 2008, *MNRAS*, **387**, 1021
 Greif T. H., White S. D. M., Klessen R. S., Springel V., 2011, *ApJ*, **736**, 147
 Gültekin K., et al., 2009, *ApJ*, **698**, 198
 Haemmerlé L., Woods T. E., Klessen R. S., Heger A., Whalen D. J., 2017, preprint, ([arXiv:1705.09301](https://arxiv.org/abs/1705.09301))
 Haiman Z., 2013, in Wiklind T., Mobasher B., Bromm V., eds, *Astrophysics and Space Science Library Vol. 396*, *Astrophysics and Space Science Library*. p. 293 ([arXiv:1203.6075](https://arxiv.org/abs/1203.6075)), doi:10.1007/978-3-642-32362-1_6
 Haiman Z., Loeb A., 2001, *ApJ*, **552**, 459
 Haiman Z., Rees M. J., Loeb A., 1996, *ApJ*, **467**, 522
 Heitsch F., 2013, *ApJ*, **769**, 115
 Hirano S., Hosokawa T., Yoshida N., Umeda H., Omukai K., Chiaki G., Yorke H. W., 2014, *ApJ*, **781**, 60
 Hirano S., Hosokawa T., Yoshida N., Kuiper R., 2017, *Science*, **357**, 1375
 Hirano S., Yoshida N., Sakurai Y., Fujii M. S., 2018, *ApJ*, **855**, 17
 Hosokawa T., Omukai K., Yoshida N., Yorke H. W., 2011, *Science*, **334**, 1250
 Hosokawa T., Omukai K., Yorke H. W., 2012, *ApJ*, **756**, 93
 Hosokawa T., Yorke H. W., Inayoshi K., Omukai K., Yoshida N., 2013, *ApJ*, **778**, 178
 Inayoshi K., Haiman Z., 2014, *MNRAS*, **445**, 1549

- Inayoshi K., Omukai K., 2011, *MNRAS*, **416**, 2748
- Inayoshi K., Omukai K., 2012, *MNRAS*, **422**, 2539
- Inayoshi K., Tanaka T. L., 2015, *MNRAS*, **450**, 4350
- Inayoshi K., Hosokawa T., Omukai K., 2013, *MNRAS*, **431**, 3036
- Inayoshi K., Omukai K., Tasker E., 2014, *MNRAS*, **445**, L109
- Inayoshi K., Visbal E., Kashiyama K., 2015, *MNRAS*, **453**, 1692
- Inayoshi K., Haiman Z., Ostriker J. P., 2016, *MNRAS*, **459**, 3738
- Inoue A. K., 2011, *MNRAS*, **415**, 2920
- Jeon M., Besla G., Bromm V., 2017, *ApJ*, **848**, 85
- Jiang L., et al., 2016, *ApJ*, **833**, 222
- Johnson J. L., 2010, *MNRAS*, **404**, 1425
- Johnson J. L., Haardt F., 2016, *Publ. Astron. Soc. Australia*, **33**, e007
- Johnson J. L., Dalla V. C., Khochfar S., 2013, *MNRAS*, **428**, 1857
- Kereš D., Katz N., Weinberg D. H., Davé R., 2005, *MNRAS*, **363**, 2
- Kitayama T., Yoshida N., 2005, *ApJ*, **630**, 675
- Klessen R. S., Hennebelle P., 2010, *A&A*, **520**, A17
- Kormendy J., Ho L. C., 2013, *ARA&A*, **51**, 511
- Koushiappas S. M., Bullock J. S., Dekel A., 2004, *MNRAS*, **354**, 292
- Larson R. B., 1969, *MNRAS*, **145**, 271
- Latif M. A., Bovino S., Van Borm C., Grassi T., Schleicher D. R. G., Spaans M., 2014, *MNRAS*, **443**, 1979
- Latif M. A., Bovino S., Grassi T., Schleicher D. R. G., Spaans M., 2015, *MNRAS*, **446**, 3163
- Latif M. A., Schleicher D. R. G., Hartwig T., 2016a, *MNRAS*, **458**, 233
- Latif M. A., Omukai K., Habouzit M., Schleicher D. R. G., Volonteri M., 2016b, *ApJ*, **823**, 40
- Lodato G., Natarajan P., 2006, *MNRAS*, **371**, 1813
- Loeb A., Rasio F. A., 1994, *ApJ*, **432**, 52
- Madau P., Haardt F., Dotti M., 2014, *ApJ*, **784**, L38
- Magorrian J., et al., 1998, *AJ*, **115**, 2285
- Mandelker N., van Dokkum P. G., Brodie J. P., van den Bosch F. C., Ceverino D., 2017, preprint, ([arXiv:1711.09108](https://arxiv.org/abs/1711.09108))
- Marigo P., Girardi L., Chiosi C., Wood P. R., 2001, *A&A*, **371**, 152
- Matsuoka Y., et al., 2016, *ApJ*, **828**, 26
- Matsuoka Y., et al., 2018, *PASJ*, **70**, S35
- Mayer L., Kazantzidis S., Escala A., Callegari S., 2010, *Nature*, **466**, 1082
- Mayer L., Fiacconi D., Bonoli S., Quinn T., Roškar R., Shen S., Wadsley J., 2015, *ApJ*, **810**, 51
- McKee C. F., Tan J. C., 2008, *ApJ*, **681**, 771
- Mo H. J., Mao S., White S. D. M., 1998, *MNRAS*, **295**, 319
- Montero P. J., Janka H.-T., Müller E., 2012, *ApJ*, **749**, 37
- Mortlock A., Conselice C. J., Bluck A. F. L., Bauer A. E., Grützbauch R., Buitrago F., Ownsworth J., 2011, *MNRAS*, **413**, 2845
- Nakamura F., Umemura M., 2001, *ApJ*, **548**, 19
- Nakamura F., Umemura M., 2002, *ApJ*, **569**, 549
- Ocvirk P., Pichon C., Teyssier R., 2008, *MNRAS*, **390**, 1326
- Oh S. P., Haiman Z., 2002, *ApJ*, **569**, 558
- Oh S. P., Haiman Z., Rees M. J., 2001, *ApJ*, **553**, 73
- Omukai K., 2001, *ApJ*, **546**, 635
- Omukai K., Schneider R., Haiman Z., 2008, *ApJ*, **686**, 801
- Ostriker J., 1964, *ApJ*, **140**, 1056
- Pacucci F., Ferrara A., 2015, *MNRAS*, **448**, 104
- Pawlik A. H., Milosavljević M., Bromm V., 2011, *ApJ*, **731**, 54
- Penston M. V., 1969, *MNRAS*, **144**, 425
- Pezzulli E., Valiante R., Schneider R., 2016, *MNRAS*, **458**, 3047
- Planck Collaboration XVI et al. 2014, *A&A*, **571**, A16
- Rees M. J., Ostriker J. P., 1977, *MNRAS*, **179**, 541
- Regan J. A., Johansson P. H., Haehnelt M. G., 2014, *MNRAS*, **439**, 1160
- Sakurai Y., Vorobyov E. I., Hosokawa T., Yoshida N., Omukai K., Yorke H. W., 2016a, *MNRAS*, **459**, 1137
- Sakurai Y., Inayoshi K., Haiman Z., 2016b, *MNRAS*, **461**, 4496
- Schauer A. T. P., Regan J., Glover S. C. O., Klessen R. S., 2017, *MNRAS*, **471**, 4878
- Shang C., Bryan G. L., Haiman Z., 2010, *MNRAS*, **402**, 1249
- Sheth R. K., Tormen G., 2002, *MNRAS*, **329**, 61
- Shibata M., Shapiro S. L., 2002, *ApJ*, **572**, L39
- Shu F. H., 1977, *ApJ*, **214**, 488
- Smidt J., Whalen D. J., Johnson J. L., Li H., 2017, preprint, ([arXiv:1703.00449](https://arxiv.org/abs/1703.00449))
- Smith B. D., Wise J. H., O'Shea B. W., Norman M. L., Khochfar S., 2015, *MNRAS*, **452**, 2822
- Spitzer Jr. L., 1942, *ApJ*, **95**, 329
- Stacy A., Bromm V., Loeb A., 2011, *ApJ*, **730**, L1
- Sugimura K., Omukai K., Inoue A. K., 2014, *MNRAS*, **445**, 544
- Sugimura K., Hosokawa T., Yajima H., Omukai K., 2017, *MNRAS*, **469**, 62
- Sugimura K., Hosokawa T., Yajima H., Inayoshi K., Omukai K., 2018, preprint, ([arXiv:1802.07264](https://arxiv.org/abs/1802.07264))
- Takeo E., Inayoshi K., Ohsuga K., Takahashi H. R., Mineshige S., 2018, *MNRAS*, **476**, 673
- Tanaka T., Haiman Z., 2009, *ApJ*, **696**, 1798
- Tanaka T. L., Li M., 2014, *MNRAS*, **439**, 1092
- Tanaka T. L., Li M., Haiman Z., 2013, *MNRAS*, **435**, 3559
- Truelove J. K., Klein R. I., McKee C. F., Holliman II J. H., Howell L. H., Greenough J. A., 1997, *ApJ*, **489**, L179
- Tseliakhovich D., Hirata C., 2010, *Phys. Rev. D*, **82**, 083520
- Tsuribe T., Inutsuka S.-i., 1999, *ApJ*, **526**, 307
- Tumlinson J., Shull J. M., 2000, *ApJ*, **528**, L65
- Uchida H., Shibata M., Yoshida T., Sekiguchi Y., Umeda H., 2017, *Phys. Rev. D*, **96**, 083016
- Umeda H., Hosokawa T., Omukai K., Yoshida N., 2016, *ApJ*, **830**, L34
- Valiante R., Schneider R., Volonteri M., Omukai K., 2016, *MNRAS*, **457**, 3356
- Visbal E., Haiman Z., Bryan G. L., 2014, *MNRAS*, **442**, L100
- Visbal E., Bryan G. L., Haiman Z., 2017, *MNRAS*, **469**, 1456
- Volonteri M., 2012, *Science*, **337**, 544
- Volonteri M., Rees M. J., 2005, *ApJ*, **633**, 624
- Wang R., et al., 2013, *ApJ*, **773**, 44
- Wang R., et al., 2016, *ApJ*, **830**, 53
- White S. D. M., Frenk C. S., 1991, *ApJ*, **379**, 52
- White S. D. M., Rees M. J., 1978, *MNRAS*, **183**, 341
- Willott C. J., et al., 2010, *AJ*, **139**, 906
- Wise J. H., Abel T., 2008, *ApJ*, **685**, 40
- Wise J. H., Turk M. J., Abel T., 2008, *ApJ*, **682**, 745
- Wolcott-Green J., Haiman Z., Bryan G. L., 2011, *MNRAS*, **418**, 838
- Wolcott-Green J., Haiman Z., Bryan G. L., 2017, *MNRAS*, **469**, 3329
- Wu X.-B., et al., 2015, *Nature*, **518**, 512
- Yajima H., Khochfar S., 2017, *MNRAS*, **467**, L51
- Yoshida N., Abel T., Hernquist L., Sugiyama N., 2003, *ApJ*, **592**, 645
- Zackrisson E., Rydberg C.-E., Schaerer D., Östlin G., Tuli M., 2011, *ApJ*, **740**, 13
- Zhang J., Ma C.-P., Fakhouri O., 2008, *MNRAS*, **387**, L13